Acta Neuropathol (Berl) (1983) 60:113–124

Acta Neuropathologica

Ultrastructural Morphology of Amyloid Fibrils from Neuritic and Amyloid Plaques

P. A. Merz[1], H. M. Wisniewski[1], R. A. Somerville[1], S. A. Bobin[1], C. L. Masters[2], and K. Iqbal[1]

[1] Institute for Basic Research in Developmental Disabilities, 1050 Forest Hill Road, Staten Island, NY 10314, USA
[2] Dept. of Neuropathology, Royal Perth Hospital, Perth, Western Australia 6001

Summary. The structure of partially purified, CNS amyloid fibrils from three different sources have been compared by negative stain EM. The fibrils isolated from brains with senile dementia of Alzheimer type were 4–8 nm in diameter, narrowing every 30–40 nm and apparently composed of two 2–4 nm filaments. The fibrils from a Gerstmann-Sträussler syndrome brain were 7–9 nm in diameter, narrowing every 70–80 nm and with a suggestion that they are composed of two 3–5 nm filaments. The fibrils isolated from 87V scrapie-affected mouse brains were 4–8 nm in diameter with a twist every 15–25 nm presumably composed of two 2–4 nm filaments. The fibrils from the scrapie brains were usually observed in pairs. The shape of the clusters of the isolated amyloid fibrils observed in each disease was similar in negative stain and thin section EM preparations and was related to the characteristic morphology of the amyloid fibrils in the neuritic and amyloid plaques in situ. The structural differences between the CNS amyloid fibrils from the various diseases studied by us may reflect differences in the polypeptides which comprise the fibril and/or a different pathogenesis in the formation of the amyloid fibrils.

Key words: Amyloid – Alzheimers disease – Scrapie – EM – Isolation – Gerstmann-Sträussler syndrome

Introduction

Neuritic and amyloid plaques are one of the most common neuropathologic changes observed in normal aged human and animal population (Wisniewski et al. 1970, 1973; Wisniewski and Terry 1976; Vaughan and Peters 1981). They are particularly common in people with the clinical diagnosis of senile dementia of the Alzheimer type (SDAT) (Wisniewski and Terry 1973). The neuritic and amyloid plaques are also observed in Downs syndrome, kuru, some cases of Creuzfeldt-Jakob disease (CJD) and Gerstmann-Sträussler syndrome (GSS) (Jervis and Soltz 1936; Klatzo et al. 1959; Beck and Daniel 1979; Schlote et al. 1980; Masters et al. 1981). Two varieties of plaques have been described which are primarily observed in light microscopy with Congo red staining and silver impregnation methods with periodic acid Schiff (PAS) staining. Neuritic plaques, found predominantly in Alzheimer's disease and SDAT, have varying degrees of amyloid deposition from the primitive plaque with the least quantity of amyloid through the classical senile plaque to the burned out amyloid plaque (Wisniewski et al. 1981a, b). Plaques observed in kuru, CJD, and GSS are composed of amyloid fibrils primarily in the form of amyloid plaques. Electron microscopy (EM) of the neuritic and amyloid plaques has demonstrated that the PAS-stained and congophilic material is composed of 6–11 nm fibrils, which have similar characteristics to the amyloid deposits observed in the generalized systemic amyloidosis (Terry and Wisniewski 1970; Wisniewski et al. 1981b; Glenner and Page 1976).

Kuru and CJD have been shown to be caused by slow viruses similar to scrapie (Gajdusek 1977). The clinical symptoms and neuropathology of kuru and CJD in experimentally infected animals parallels the clinical course and neuropathology of the human diseases. Status spongiosis is the primary histological feature in both the human diseases and the infected animals. However, the amyloid deposits characteristic of some kuru and CJD cases were not observed in infected animals even those inoculated with material from cases known to contain amyloid plaques (Beck and Daniel 1979). GSS is a familial disease consistent with an autosomal dominant mode of inheritance. The clinical history is characterized by cerebellar signs in which some cases also exhibit dementia. The neuropathology is characterized by a spinal cerebellar degeneration with the presence of amyloid and a few

Offprint requests to: Patricia A. Merz, MD (address see above)

neuritic plaques throughout the brain. Several cases also have spongiform changes typical of CJD. A CJD-like disease appeared in primates inoculated with brain material from four cases of GSS (Master et al. 1981). Again only vacuolation and no amyloid plaques were observed in the clinically affected animals. The transmission of the sporadic or familial Alzheimer's disease to an animal host has yet to be demonstrated (Goudsmit et al. 1980; Brown et al. 1983).

Scrapie, a progressive degenerative CNS disease of sheep and goats, has been transmitted to laboratory rodents (Chandler 1963). Although vacuolation is a common neuropathologic feature of the many scrapie strains, the formation of neuritic and amyloid plaques occurs only in certain specific agent-host combinations (Bruce and Fraser 1975; Wisniewski et al. 1975; Fraser 1979). These scrapie-host combinations are the only animal models available for studying the dynamics of the neuritic and amyloid plaque formation. The amyloid deposits caused by two particular strains of scrapie (87V and 87A) appear to be locally produced within the CNS as a response to the infectious agent, particularly at the site of the injection, following intracerebral inoculation (Bruce and Fraser 1981; Wisniewski et al. 1981a, b).

The amyloid fibrils isolated from the various systemic amyloidoses are straight and unbranched but vary somewhat in their detailed ultrastructure. In thin section EM, the systemic amyloid fibrils have an average diameter of 10 nm with a range of 8 – 20 nm when observed in situ, isolated as plaques, or isolated with distilled water and aggregated in low salt (Pras et al. 1968; Rosenthal and Franklin 1977). Negative stain EM has been extensively employed in the morphological characterization of the amyloid fibrils after demonstration of the solubility of the amyloid fibril in distilled water and its re-aggregation with the addition of low salt (Shirahama and Cohen 1965; Pras et al. 1968; Rosenthal and Franklin 1977). The re-aggregated fibrils in low salt are generally observed as clusters of fibrils, in which each fibril appears to be composed of two or more filaments each 5 – 7 nm in diameter. The 5 – 7 nm filament is reported to be composed of two protofilaments 2.5 – 3.5 nm in diameter (Shirahama and Cohen 1965).

In this paper we describe the negative stain morphology of three types of partially purified CNS amyloid from Alzheimer's disease, GSS, and 87V scrapie and discuss the differences observed.

Materials and Methods

Materials

Alzheimer Disease. The brains from three morphologically confirmed cases of SDAT were used. The morphological studies revealed the presence of predominantly primitive neuritic plaques in all three cases. Before amyloid isolation, samples of the individual brains were frozen at – 70° C for periods of up to 3 years.

Gerstmann-Sträussler Syndrome (GSS). This case originated in a family exhibiting autosomal-dominant mode of inheritance of GSS in which four generations had been affected. The clinical course of this case (Masters et al. 1981, Fig. 2, Case IV-2) was a neurologic disease (cerebellar degeneration) with dementia. Neurologic examination after autopsy showed amyloid and some neuritic plaques throughout the brain and spongiform encephalopathic changes similar to CJD. The studied samples of the cortex were frozen at – 70° C until used.

Control Material. One human brain without a neurologic history and not having amyloid or neuritic plaques demonstrable on routine neuropathologic examination of sections stained with Bodian-PAS or Congo red was processed for amyloid fibrils to determine whether the use of the chemical procedures can produce fibres of the amyloid type. Samples of brain were frozen at – 70° C.

87V Scrapie. Weanling IM/Dk mice were inoculated intracerebrally in the right hemisphere with 1% homogenate of 87V scrapie-infected VM mouse brain. Clinical disease appeared about 9 months after inoculation. Animals for amyloid isolation were killed by cervical dislocation. The brains were removed and frozen at – 70° C. One animal in six was perfused with 3% glutaraldehyde in 0.1 M Sorenson's buffer (Vorbrodt et al. 1981). Its brain was removed and processed for histopathology. Histopathology confirmed the presence of periventricular and cortical amyloid and neuritic plaques following Congo red, Masson trichrome, or Bodian PAS staining.

Control Mice. Weanling mice of IM/Dk strain were inoculated intracerebrally in the right hemisphere with 1% normal brain homogenate of the corresponding mouse strain. Animals, age-matched to the scrapie-inoculated IM/Dk mice, were killed by cervical dislocation, the brains removed and frozen at – 70° C until used. Several animals were perfused with 3% glutaraldehyde in 0.1 M Sorenson's buffer (Vorbrodt et al. 1981), brains were removed and processed for histopathology. Following Congo red, Masson trichrome, or Bodian PAS staining, microscopic studies of these brains did not reveal amyloid plaques.

Methods

Amyloid Preparation. The entire isolation procedure is carried out at 4° C except where indicated. Single frozen mouse brains or 1 – 10 g of human frozen cerebral cortex, dissected free of white matter, were minced and homogenized in 10 vol. of 0.1 M acetate buffer, pH 4.5 using a Dounce homogenizer with a loosely fitting pestle. The homogenate was centrifuged at 2,400 *g* for 15 min at which point one of the three following procedure was performed:

(1) The pellet was treated with 1% Triton X-100, 1% urea, and 1% sodium dodecylsulfate and centrifuged at 2,400 *g* for 15 min. The resulting pellet was examined by negative stain EM after dilution with distilled water.

(2) The pellet from 1 was suspended in 0.5 M sucrose and layered over a 1 – 1.5 M sucrose gradient and centrifuged at 100,000 *g* for 2 h. Aliquots from the fractions of the gradient were diluted with distilled water and examined by negative stain EM.

(3) The original pellet was resuspended in 2% pepsin in 0.1 M acetate buffer pH 4.5 and incubated at 37° C for 30 min. The suspension was sonicated with a Branson microprobe at full strength for 15 s and reincubated with 2% pepsin for another 30 min, then centrifuged at 8,000 *g* for 15 min. The suspension was sonicated with a Branson microprobe at full strength for 15 s and re-incubated with 2% pepsin for another 30 min, then centrifuged at 8,000 *g* for 15 min. The pellet was treated with 2% octyl glucoside in 0.32 M sucrose,

10 mM Tris-HCl, pH 7.5, and the solution layered over a 25% metrisamide in 10 mM Tris HCl, pH 7.5, pad. The amyloid fibrils were recovered in the pellet.

Congo Red Staining. An aliquot of each pellet was stained with 1% Congo red in distilled water and viewed under polarized light.

Systemic Amyloid Preparations

Control and primary amyloidosis liver (0.5 *g*) were individually homogenized in 0.32 M sucrose with a motor driven teflon-glass homogenizer. Control and secondary amyloidotic spleen were separately homogenized in 0.2 M KCl with a Dounce Homogenizer. The homogenates were spun at 1,500 *g* for 10 min. The supernates pipetted off and the pellets washed. The combined supernates were spun at 50,000 *g* for 20 min. The pellets were resuspended in 2 ml of 1% octylglucoside, 0.32 M sucrose, 10 mM Tris HCl, pH 7.5. After centrifugation in the SW 27.1 rotor at 80,000 *g* overnight the resulting pellets and interface were collected and examined by negative stain EM.

Electron Microscopy

Thin Section EM. For this study, fibrils from the three different diseases were isolated according to method 3. The preparations were centrifuged in Beem capsules at 40,000 *g* for 30 min. Pelletes were fixed in 5% glutaraldehyde in 0.1 M cacodylate buffer, pH 7.0 for 3 h, washed in buffer, postfixed with 1% buffered osmium tetroxide, dehydrated with graded alcohols, and embedded in plastic (Spurr 1969). Sections were cut on a Sorvall MT-2B Ultramicrotome and stained with aqueous uranyl acetate and lead citrate.

Negative Stain EM. All samples were coded prior to the microscopist receiving them. One drop of sample was placed for 1 min on freshly glow-discharged, carbon-coated 300- or 400-mesh grids. The sample was drained, stained for 1 min with 3% phosphotungstic acid (PTA) pH 7.2 (pH adjusted with NaOH), drained, and air dried. The grids were examined shortly after preparation. After examination in the Philips EM 300, the grids were stored under a vacuum. All samples were evaluated initially at ×20,540. Between 20 and 50 squares were examined for each grid and micrographs were taken from ×3,000 to ×73,000. The resolution of the microscope (as calibrated with metal shadowed latex spheres) was better than 1 nm. The samples were decoded after the microscopist had evaluated the grids for the presence of amyloid fibrils, and estimated the type of fibrils observed.

Results

SDAT Amyloid

The amyloid fibrils for the three cases of SDAT appeared straight and unbranched with a diameter of 4–8 nm when observed by negative stain EM (Fig. 1a, b). They were arranged on the grid in an ordered clump, usually triangular to rectangular in shape with the fibrils generally arrayed parallel to each other. In areas in which the fibrils were lightly stained, they appeared to be twisted with a narrowing to 2–4 nm every 30–40 nm. Occasionally, two filaments were observed to comprise the amyloid fibril with each filament being 2–4 nm in diameter (Fig. 1c).

If the detergent treatment was omitted, the amyloid fibrils were not readily observed. Occasionally, large areas of fibrillar structures could be observed in negatively stained preparations during the development of the concentrations of detergent to be used. However, the detail of these fibers could not be resolved because of the apparently proteinaceous material in which the fibers were enmeshed (Fig. 2).

The fibrils were observed under all methods of preparation. Two or more amyloid clusters per grid-square were observed in all three methods of preparation. On occasion, paired helical filaments of the Alzheimer type (PHF) were also observed in these samples. Dispersed single amyloid fibrils were not seen in these preparations.

The identification of the negatively stained fibrils as amyloid was confirmed by thin section EM (Fig. 3a, b). The fibrils were observed in parallel arrays with the same general shape as that observed in negative stain. They were surrounded by a light staining granular material which made it hard to delineate the exact dimensions of the individual fibrils. The width of the fibrils when measured in optimal conditions was 4–8 nm.

Contaminants were densely stained small irregular aggregates, some collagen, and membraneous debris. Green-red birefringent amyloid material was not observed by light microscopy after Congo red staining of the detergent isolated suspension.

GSS Amyloid

In contrast to the preparations from SDAT relatively few amyloid fibrils were seen as clusters by negative stain EM. In the preparations of GSS amyloid about one area of loose fibrils per grid square appeared as a small cluster with 5–10 amyloid fibrils radiating outward from the center of the cluster (Fig. 4a). The fibrils were straight and unbranched. They measured 7–9 nm at their widest narrowing to 3–5 nm every 70–80 nm (Fig. 4b). At high magnification the GSS amyloid fibril appears to be composed of two filaments, each 3–5 nm in diameter. The staining of the wide portion and the narrow portion was even, revealing no differences in substructure.

Large dark profiles, presumably the amyloid stars which occupied almost a whole square were observed in these preparations but no detail could be observed due to their size. Amyloid was observed in three different preparations using method 3 and the morphology of the fibrils did not vary. When the detergent was omitted from the isolation procedure individual amyloid fibrils were not observed.

Thin section EM of the pellets revealed large amyloid cores which were presumably the large dark structures in negative stain (Fig. 5a, c). Two types of amyloid cores were observed in the GSS preparations. One type was free of cellular debris and the fibrils were

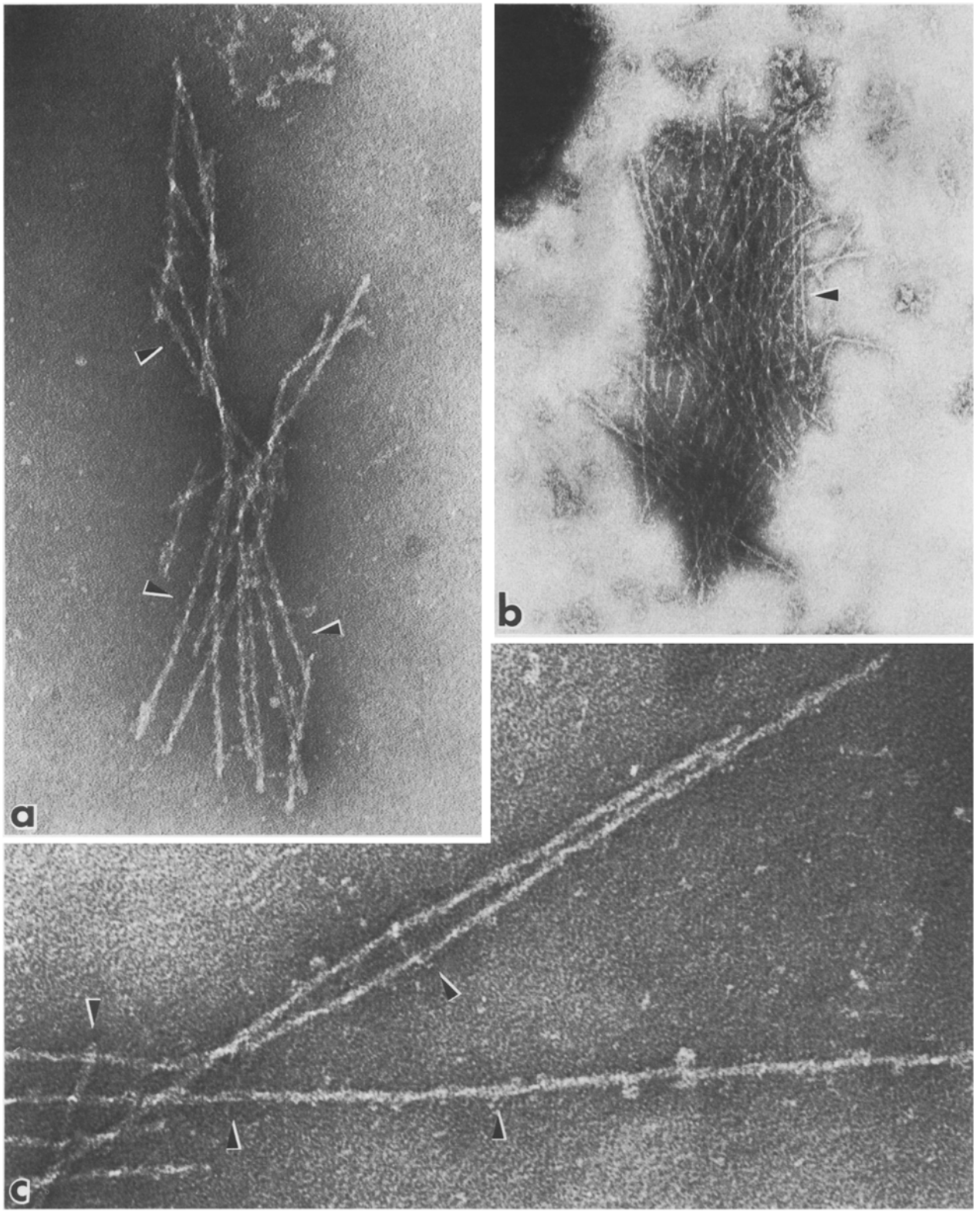

Fig. 1 a–c. Micrographs of negatively stained amyloid fibrils from SDAT brains. **a** Amyloid fibrils from SDAT case 2 prepared by method 1, note the distinct narrowing every 30–40 nm of the 4–8 nm fibrils, × 166,000. **b** Amyloid fibrils from SDAT case 1 prepared by methods 3. Even at this magnification the helical nature of the individual fibrils is apparent (→), × 74,500. **c** Amyloid fibrils from SDAT case 2 prepared by method 2, note the distinct protofilaments (→), ×300,000. All are stained with 3% PTA

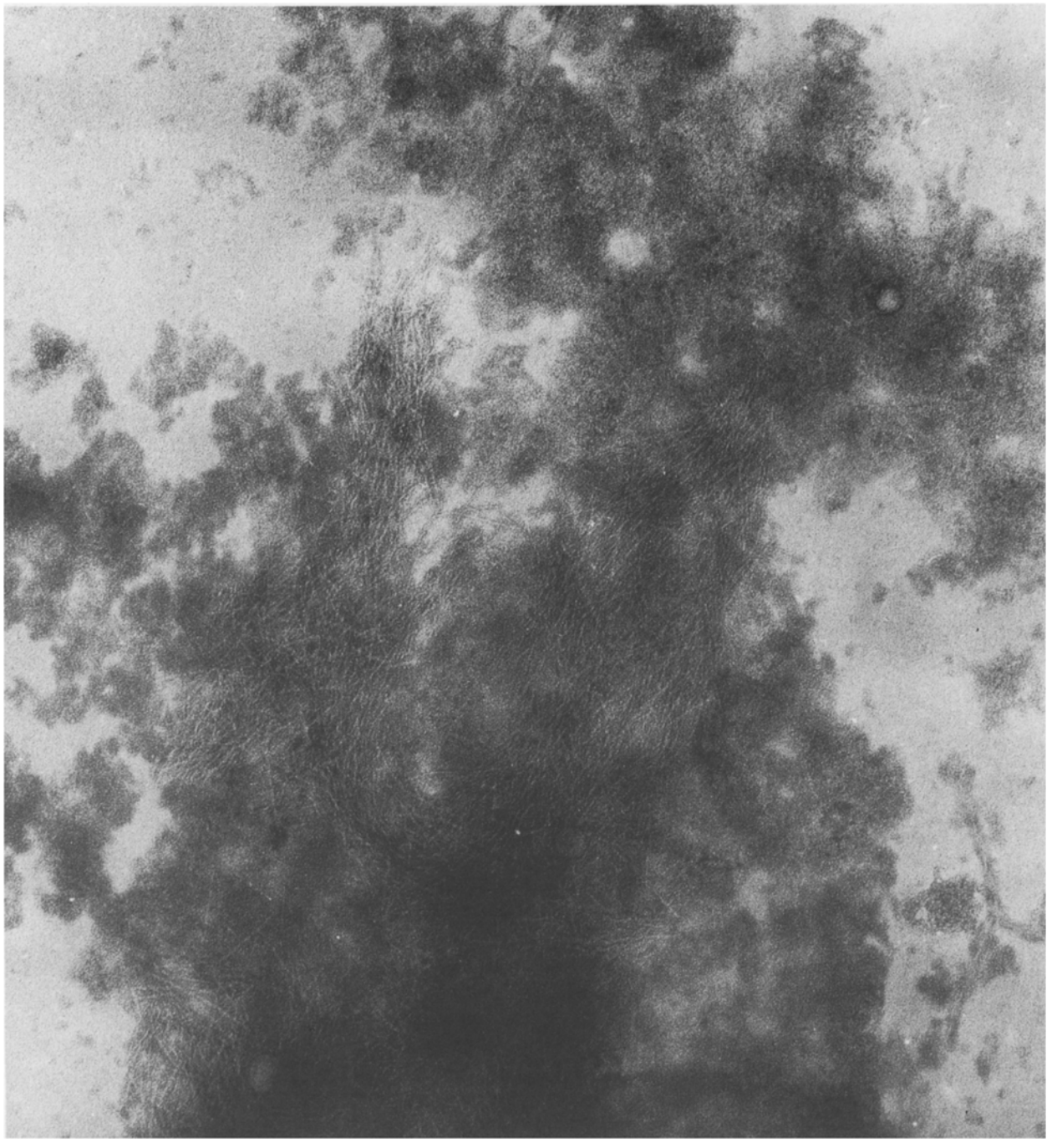

Fig. 2. Negatively stained preparation of amyloid fibrils from SDAT prepared with low concentrations of Triton X-100 in which the fibrils are deeply enmeshed in an amorphous protein-like material. Structural details of the fibrils cannot be observed. Stained with 3% PTA, × 86,000

loosely packed. The second one was associated with amorphous cellular debris and the fibrils were tightly packed in cable-like structures. The fibrils of the first type were easily stained and the edges readily delineated similar to the loose individual fibrils observed. They were 6–10 nm in diameter, and debris was not associated with them. Hints of the 10 nm fibril being composed of two filaments were observed as a dark line in the center of a 10 nm filament (Fig. 5c). The plaques associated with cellular debris had a starburst appearance (Fig. 5b), but within the starburst were darkly stained irregular aggregates of amorphous material.

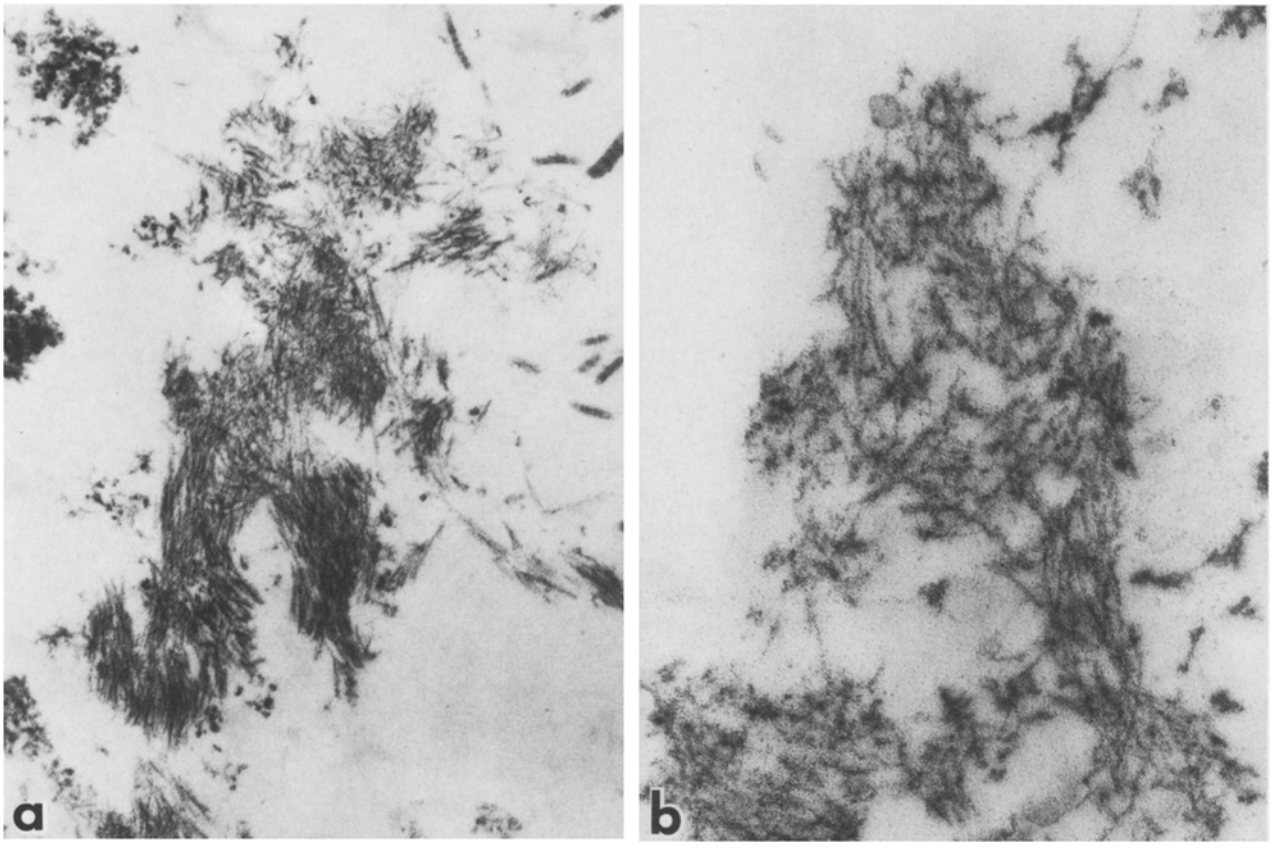

Fig. 3a, b. Micrographs of thin sections of embedded SDAT amyloid fibrils prepared by method 3. **a** At low magnification with some of the contaminants, × 43,000. **b** At higher magnification illustrating the fibrillar character, dimensions and lightly staining material between the fibrils, × 80,000. All are stained with uranyl acetate and lead citrate

The fibrils in these plaques were in tightly packed clusters, and it was difficult to obtain the individual measurement of the fibrils (Fig. 5d). Those measureable were 6–8 nm in diameter.

The contaminants observed in these preparations were collagen, densely stained irregular globular aggregates, and large membranous debris. A large concentration of classic green-red birefringent amyloid cores was observed by light microscopy with Congo red staining of the detergent isolated suspension.

87V Scrapie Amyloid

Fibrils were observed by negative stain EM when individual brains of mice, clinically affected with 87V scrapie, were prepared by method 3. Two forms of fibril were observed. A few individual fibrils were seen distributed randomly on squares of the grid. These fibrils were similar to scrapie associated fibrils (SAF) seen in other scrapie agent-host combinations (Merz et al. 1981). The second form of fibril was found in small clusters (Fig. 6a) which appeared flat and oblong. The diameter of the fibrils was 4–8 nm. High resolution EM suggests that each 4–8 nm fibril is twisted every 15–25 nm (Fig. 6b). This observation suggests a substructure of 2–4 nm filaments, but further substructural analysis was not possible. These fibrils were usually seen as straight pairs with a diameter of 11–20 nm.

The small plaque-like structures were seen about once every 5 squares of the grid. Often these structures were observed emerging from or adhering to a mass of unidentified amorphous material. When amyloid was prepared by method 2 only the plaque-like structures were observed and not the individual fibrils similar to the SAF. Again amyloid (individual or clustered) fibrils were not observed when the detergent treatment was omitted.

Thin section EM of the pellets revealed fibrils in a loose random arrangement (Fig. 7a, b). Most of the fibrils measured an average of 6 and 12 nm in diameter. Presumably the 6 nm fibrils are the 4–8 nm fibril observed in negative stain preparations and the 12 nm fibrils are a pair of the 4–8 nm fibrils observed as the 11–20 nm fibrils in negative stain preparations.

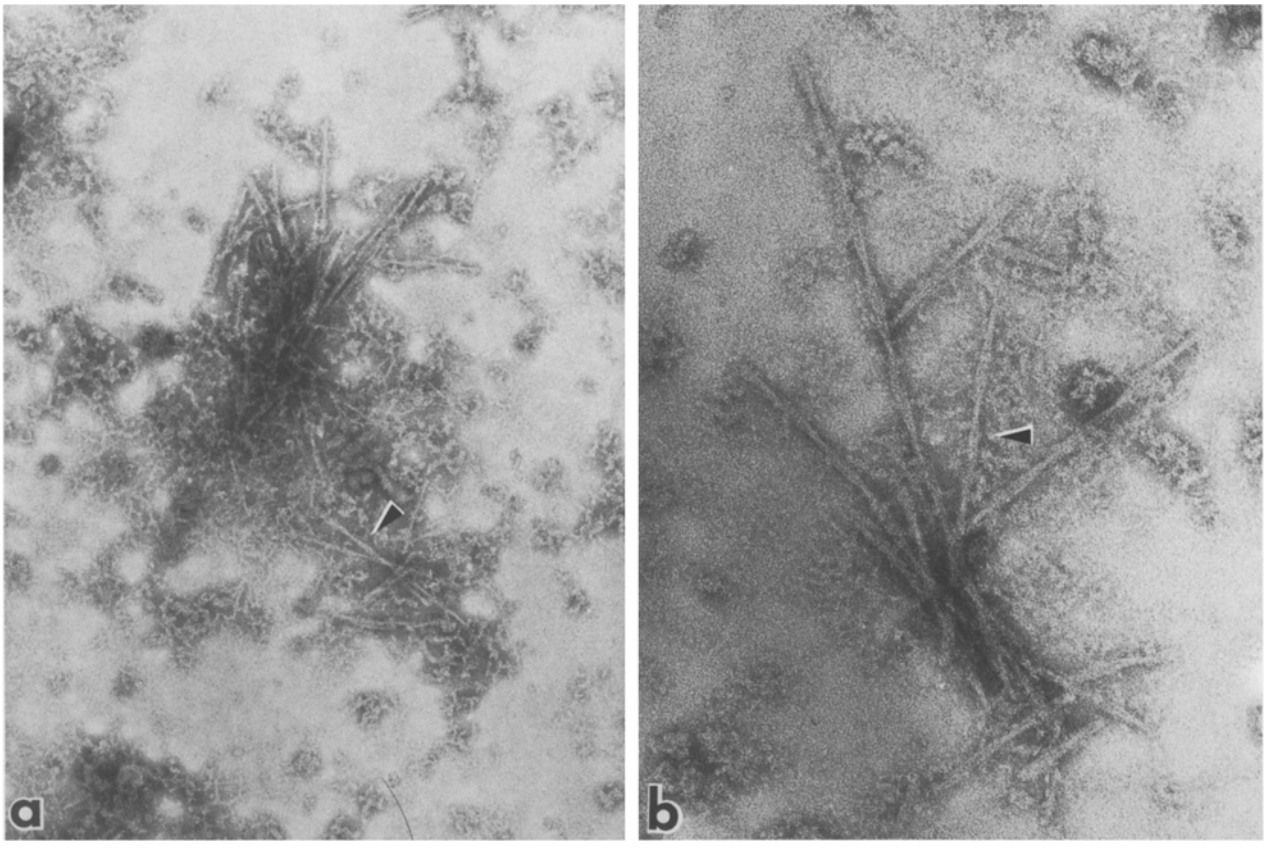

Fig. 4a, b. Negatively stained preparations of amyloid fibrils from the GSS case prepared by method 3. **a** At low magnification of the fibrils indicating the clustering observed and the helical nature of the fibrils (→), × 74,000. **b** At high magnification the distinct helical nature of the narrowing every 70 – 80 nm can be observed plus the suggestion of two protofilaments, 3 – 5 nm in diameter (→), × 164,000. All are stained with 3% PTA

The contaminants observed were similar to those seen in the preparations from human brains. Green-red birefringent material was not observed under light microscopy with Congo red staining of the detergent treated suspension.

Control Material

One human brain (17 years old) without amyloid deposition on neuropathologic examination at autopsy was processed once using method 2 and twice by method 3. Six different series of experiments with normal mouse brains were processed by method 2 (three times) and method 3 (three times). In all cases green-red birefringent material was not observed under polarized light and amyloid-like fibrils were not observed under negative stain EM.

Systemic Amyloid

The amyloid fibrils observed in the preparations from the primary amyloidosis liver was seen as a pair, 6 – 10 nm in diameter (Fig. 8a). Each filament measured 3 – 5 nm in diameter and was 50 – 100 nm in length. The internal structure of each filament could not be resolved. The amyloid fibrils observed in the preparations from the secondary amyloidosis spleen were seen as individual fibrils measuring 7 – 9 nm in diameter, narrowing to 3 – 5 nm every 70 nm. Their helical appearance suggests that they are composed of two filaments (Fig. 8a). In both these preparations a large number of fibrils were observed in each square of the grid. Besides a few collagen fibrils, the amyloid fibrils were the major structural element observed. Control preparations did not contain amyloid fibrils, but did contain large amorphous aggregates and some collagen fibrils.

Discussion

All the negatively stained fibrils observed were straight and unbranched 4 – 9 nm fibrils, helically wound with a differing periodicity. However, the morphology of the individual amyloid fibrils, isolated under these conditions, differed in the three CNS diseases as observed

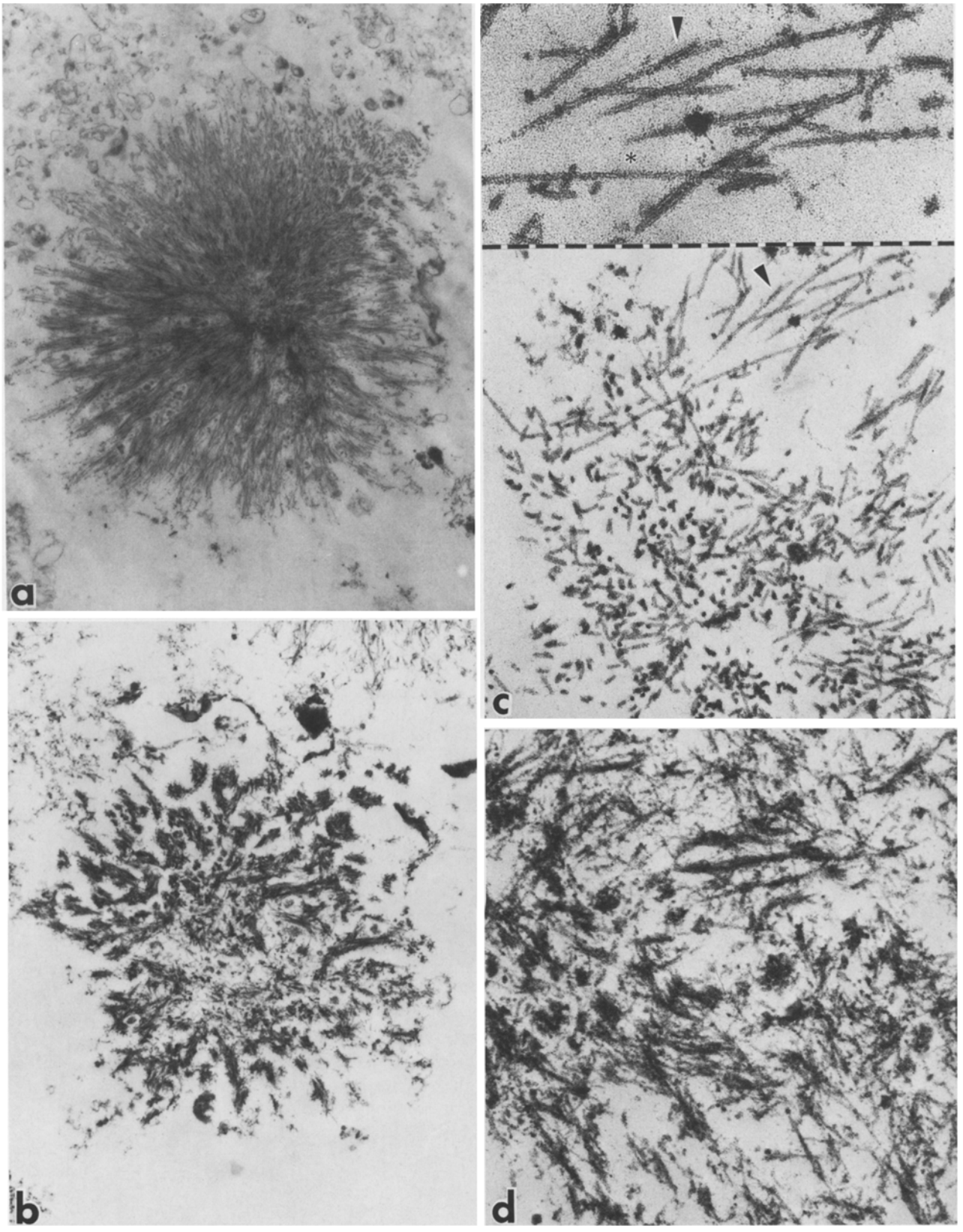

Fig. 5a–d. Micrographs of thin sections of embedded amyloid fibrils from the GSS case prepared by method 3. **a** An amyloid core in which individual fibrils radiate from the center and each fibril is clearly observed, × 12,000. **b** An amyloid core in which the fibrils can be observed as thick bundles, × 15,000. **c** Loose amyloid fibrils not in a core arrangement, in which well defined edges are seen; the fibrils measure 7–9 nm in diameter, and apparent cross-sections are present, × 69,000. The helical nature of the fibrils can be observed at the arrow and star (inset: × 143,000). **d** The fibrillar nature of the densely packed plaque at higher magnification in which the fibrils are difficult to measure, × 68,500. All are stained with uranyl acetate and lead citrate

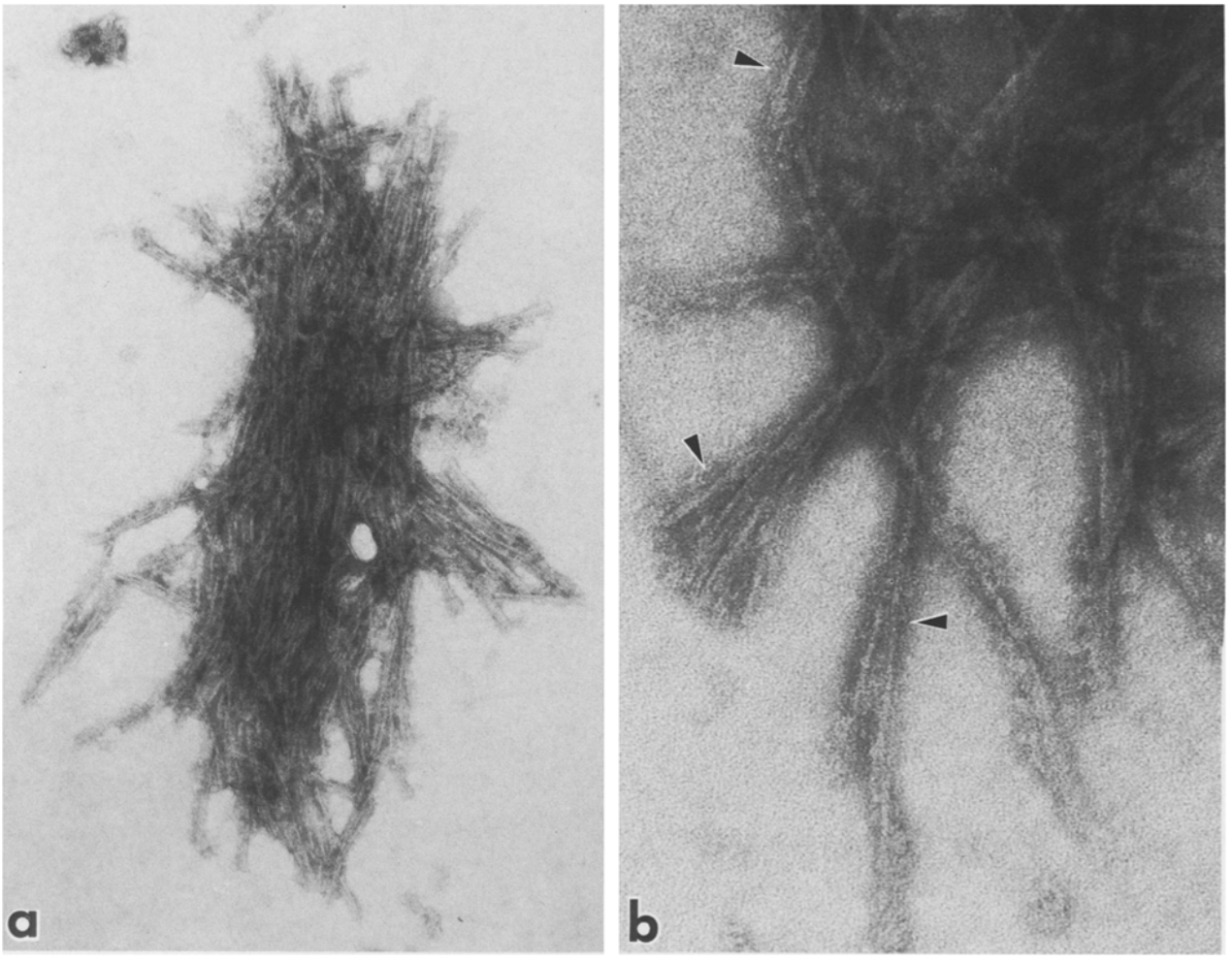

Fig. 6a, b. Negatively stained preparations of amyloid fibrils from 87 V affected IM mouse brains prepared by method 3. **a** Low magnification of a typical arrangement of the amyloid fibrils with the fibrils occurring primarily as pairs, × 90,000. **b** A high magnification view of the amyloid fibrils indicating the structure of the individual 4–8 nm fibrils. An apparent twist can be observed every 15–25 nm (→), × 224,000. All are stained with 3% PTA

by negative stain EM (Table 1). The amyloid fibril observed in the SDAT preparations measured 4–8 nm in diameter at its widest narrowing to 2–4 nm every 30–40 nm. This fibril appeared to be composed of two filaments, each filament being 2–4 nm in diameter. The helical nature of the negatively stained amyloid fibrils has previously been observed in studies on thin sections of Alzheimer amyloid fibrils with tilting of the sample (Narang 1980). The GSS amyloid fibril measured 7–9 nm in diameter, narrowing to 3–5 nm in diameter. The 87 V scrapie amyloid fibril is 4–8 nm in diameter and usually observed as pairs. The individual fibril apparently has a twist every 15–25 nm with the appearance of a twisted ribbon.

These CNS amyloids show a morphological resemblance to the published descriptions of the negatively stained, isolated, systemic amyloid fibrils. They all have a rigid appearance, are unbranched and the individual fibrils measure 4–10 nm in diameter. The protein AA fibrils we have prepared are similar to the published micrographs of protein AA fibrils of Familiar Mediterranean Fever (Glenner et al. 1974) and to the fibrils observed in the GSS preparations. The primary amyloidosis fibrils we have observed are similar to the published micrographs of primary IgG amyloid fibrils (Glenner et al. 1974; Pras et al. 1968), and the amyloid fibrils observed in 87 V mouse brain preparations. The Alzheimer fibril is similar to the metal shadowed amyloid fibrils (Sorenson and Finke 1968). Polypeptide analysis of CNS amyloid fibrils would greatly help in further delineating these relationships.

Thin section EM revealed a consistent picture of amyloid fibrils being 6–10 nm in diameter from each

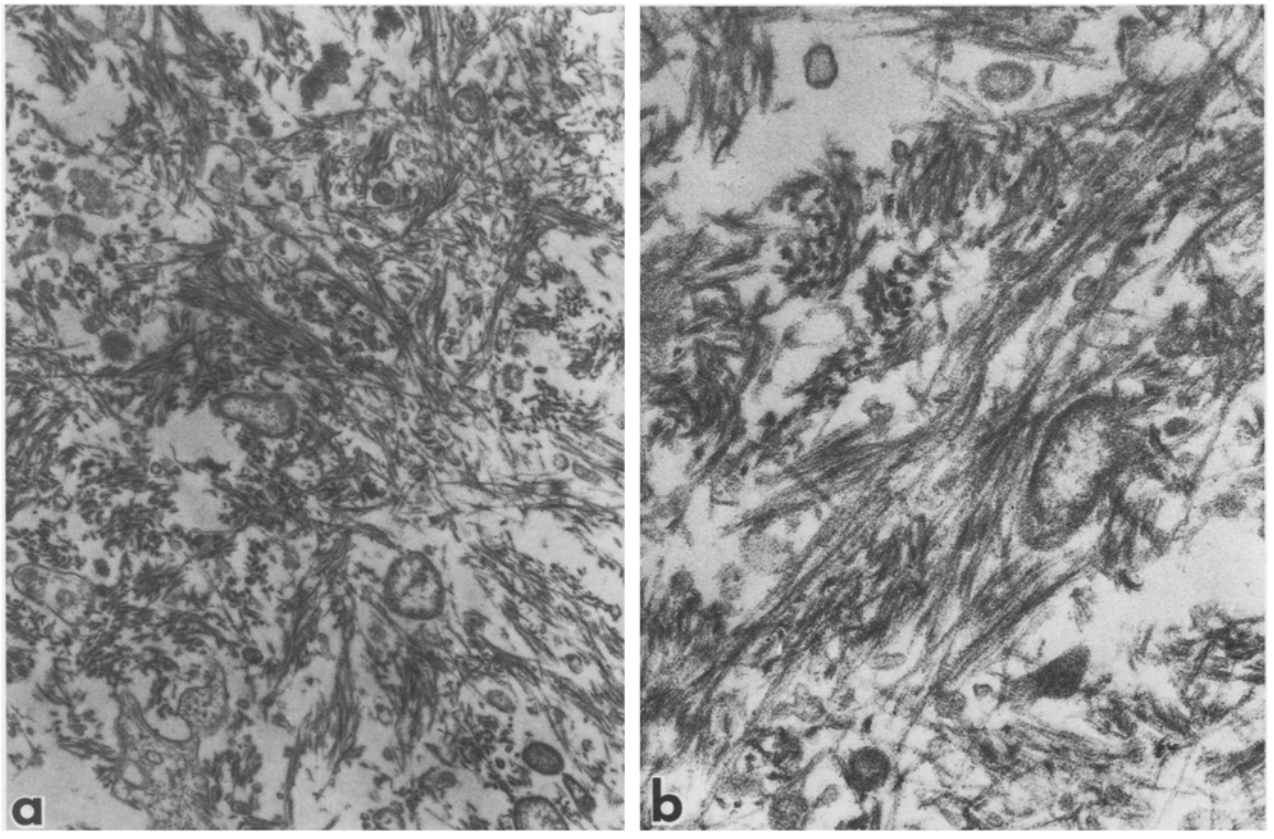

Fig. 7a, b. Micrographs of thin sections of embedded amyloid fibrils from 87 V affected mouse brains prepared by method 3. **a** An illustration of the haphazard arrangement of the amyloid fibrils and some of the debris associated with them, × 22,000. **b** A high magnification view of the amyloid fibrils illustrating cross sections, individual fibrils (4–8 nm) and pairs, × 59,000. All are stained with uranyl acetate and lead citrate

of three CNS diseases studies. They are similar in the apparent rigidity and size but they differ in the arrangement of the fibrils. The GSS amyloid fibrils are seen primarily as stellate cores with a difference in the staining of the individual fibrils. The Alzheimer fibrils are aligned in a parallel array and the 87 V amyloid fibrils are in a haphazard arrangement. This could reflect possible different polypeptides composing the fibrils or possible different methods in the secretion of the amyloid precursor protein or the polymerization of the amyloid fibril.

The isolation procedure used in this study differs in the procedures employed from those being developed to isolate amyloid cores from amyloid plaques.

The use of detergent in this procedure allows the visualization of the wisps of amyloid fibrils of the primitive plaques without a central core of amyloid. From pilot studies (Fig. 2), it became apparent that the majority of the amyloid fibrils are enmeshed in amorphous material. This may help to explain the conflicting immunochemical data such as positive staining for prealbumin, albumin, gamma globulin, neurofilament polypeptides and complements (Eikelboom and Stam 1982; Powers et al. 1981, Shirahama et al. 1982; Wisniewski and Kozlowski 1982).

Amyloid cores could only be visualized by Congo red staining in preparations from the GSS brain where characteristic green/red birefringence was observed with polarized light. It was possible to use the Congo red method to monitor the isolation of amyloid only in the GSS case in which the neuropathology had shown the presence of a large number of kuru type plaques. The negative stain EM technique was more useful in detecting the amyloid fibrils, and revealing the differing infrastructure in the diseases studied than routine thin section EM.

In summary, the partially purified amyloid fibrils isolated from the three CNS diseases showed a consistent protofilament structure. The differing dimensions and periodicity of the helix in the diseases may be based on the interactions of the protofilaments with each other, a differing polypeptide composition or differences in the pathogenetic mechanisms generating the fibrils. To resolve this problem, purification of the fibrils, followed by the polypeptide analysis and antibody studies will be necessary.

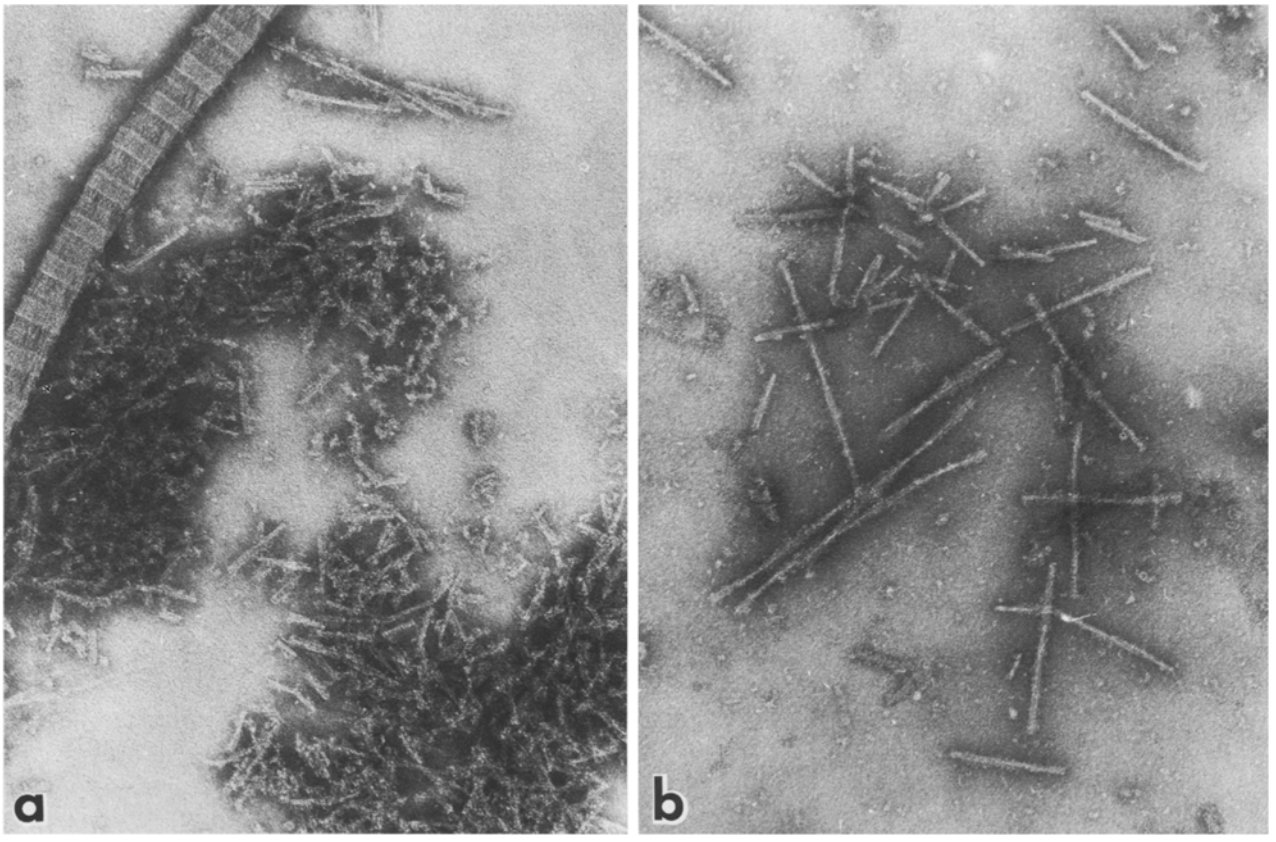

Fig. 8a, b. Negatively stained preparations of systemic amyloid fibrils prepared as described in methods, × 106,000. **a** Amyloid fibrils from primary amyloidosis liver, composed of a portion of the immunoglobulin light chain and observed primarily as short pairs. A collagen fiber is also observed. **b** Secondary amyloid fibrils composed of protein AA from spleen. The helical nature of the fibrils can easily be observed. The two systemic amyloid fibrils are distinct from each other in dimensions and morphology. All are stained with 3% PTA

Table 1. Negative stain ultrastructural characteristics of isolated amyloid fibrils

Source of amyloid fibril		Diameter (nm)	Distance between twists	Single filament diameter (nm)	Comments
CNS	AD/SDAT	4–8	30–40	2–4	
	GSS	7–9	70	3–5	
	87V	4–8	15–25	2–4	Observed as straight pairs 10–20 nm in width
Systemic	AA	7–9	70	3–5	
	AL	3–5	?	3–5	Observed as short pairs 8–12 nm in width

Acknowledgements. We wish to thank our colleagues for their generous support, in particular Dr. R. Rudelli of this Institute and Dr. G. Magolis, Dartmouth Medical School, NH, for two of the SDAT brains; Dr. A. Dickinson, MRC and ARC Neuropathogenesis Unit, Edinburgh, Scotland, for the IM/Dk mice and the 87 V strain of the scrapie agent; Dr. E. Benditt and Dr. E. Nielsen, University of Washington, for the systemic amyloidosis and control livers and spleens; Dr. G. Merz, and Dr. R. Kascsak for their encouragement, criticism and discussion, Dr. R. Moretz for discussion and preparation of the perfused mice, Ms. J. Shek for the neuropathology preparation; Ms. C. Rue for expert technical assistance, Mr. Richard Weed for photographic assistance, and Ms. Patricia Calimano for typing the manuscript.

References

Beck E, Daniel PM (1979) Kuru and Creutzfeldt-Jakob disease: neuropathological lesions and their significance. In: Prusiner SB, Hadlow WJ (eds) Slow transmissible diseases of the nervous system, vol 1. Academic Press, New York, pp 253–285

Brown P, Salazar AM, Gibbs CJ Jr, Gajdusek, DD (1982) Alzheimer's disease and transmissible virus dementia (Creutzfeldt-Jakob disease). Ann NY Acad Sci 396:131–143

Bruce ME, Fraser H (1975) Amyloid plaques in the brains of mice infected with scrapie, morphological variation and staining properties. Neuropathol Appl Neurobiol 1:189–202

Bruce ME, Fraser H (1981) Effect of route of infection on the frequency and distribution of cerebral amyloid plaques in scrapie mice. Neuropathol Appl Neurobiol 7:289–298

Chandler RL (1963) Experimental scrapie in the mouse. Res Vet Sci 4:276–285

Eikelenboom P, Stam FC (1982) Immunoglobins and complement factors in senile plaques. Acta Neuropathol (Berl) 57:235–242

Fraser H (1979) Neuropathology of scrapie: the precision of the lesions and their diversity. In: Prusiner SB, Hadlow WJ (eds) Slow transmissible diseases of the nervous system, vol 1. Academic Press, New York, pp 387–406

Gajdusek DC (1977) Unconventional viruses and the origin and disappearance of kuru. Science 197:943–960

Glenner GG, Eanes ED, Bladen HA, Finke RP, Termine JD (1974) B pleated sheet fibrils: a comparison of native amyloid fibrils with synthetic protein fibrils. J Histochem Cytochem 22:1141–1158

Glenner GG, Page DL (1976) Amyloid, amyloidosis and amyloidogenesis. In: Rechter GW, Epstein MA (eds) International review of experimental pathology, vol 15. Academic Press, New York, pp 1–92

Goudsmit J, Morrow CH, Asher DM, Yanagikara RT, Masters CL, Gibbs CJ Jr, Gajdusek DC (1980) Evidence for and against the transmissibility of Alzheimer's disease. Neurology 30:945–950

Jervis GA, Soltz SW (1936) Alzheimer's disease – the so-called juvenile type. Am J Psychiat 93:39–56

Klatzo V, Gajdusek DC, Zigas V (1959) Pathology of kuru. Lab Invest 8:799–847

Masters CL, Gajdusek DC, Gibbs CJ Jr (1981) Creutzfeldt-Jakob disease virus isolations from the Gerstmann-Sträussler syndrome: With an analysis of the various forms of amyloid plaque deposition in the virus induced spongiform encephalopathies. Brain 104:559–588

Merz PA, Somerville RA, Wisniewski HM, Iqbal K (1981) Abnormal fibrils from scrapie-infected brain. Acta Neuropathol (Berl) 54:63–74

Narang HK (1980) High resolution election microscopic analysis of the amyloid fibril in Alzheimer's disease. J Neuropathol Exp Neurol 39:621–631

Powers JM, Schlaepfer WW, Wellingham MC, Hall BJ (1981) An immunoperoxidase study of senile cerebral amyloidosis with pathogenetic consideration. J Neuropathol Exp Neurol 40:592–612

Pras M, Schubert M, Zucker-Franklin D, Rimon A, Franklin EC (1968) The characterization of soluble amyloid prepared in water. J Clin Invest 47:924–933

Rosenthal CJ, Franklin EC (1977) Amyloidosis and amyloid protein. In: Thompson R (ed) Recent advances in clinical immunology. Churchill-Livingstone, Edinburgh, pp 41–76

Schlote W, Boellaard JW, Schumm F, Stohr M (1980) Gerstmann-Sträussler Scheinkers disease: electron-microscopic observations on a brain biopsy. Acta Neuropathol (Berl) 52:203–211

Shirahama T, Cohen AS (1965) Structure of amyloid fibrils after negative staining and high resolution electron microscopy. Nature (Lond) 206:737–738

Shirahama T, Skinner M, Westermark P, Rubinow A, Cohen AS, Brun A, Kemper TL (1982) Senile cerebral amyloid prealbumin as a common constituent in the neuritic plaque, in the neurofibrillary tangle, and in the microangiopathic lesion. Am J Pathol 107:41–50

Sorenson GD, Finke E (1968) The ultrastructure of amyloid. In: Mandema E, Ruinen L, Scholten JH, Cohen AS (eds) Amyloidosis. Excerpta Medica, Amsterdam, pp 184–190

Spurr AR (1969) A low viscosity epoxy resin embedding medium for electron microscopy. J Ultrastruct Res 26:31–43

Terry RD, Wisniewski HM (1970) The ultrastructure of the neurofibrillary tangle and the senile plaque. In: Wolstenholmer GEW, O'Connor M (eds) CIBA Foundation Symposium on Alzheimer's disease and related conditions. Churchill, London, pp 145–168

Vaughan DW, Peters A (1981) The structure of neuritic plaques in the cerebral cortex of aged rats. J Neuropathol Exp Neurol 40:472–487

Vorbrodt AW, Lossinsky AS, Wisniewski HM, Moretz RC, Iwanowski L (1981) Ultrastructural cytochemical studies of cerebral microvasculature in scrapie infected mice. Acta Neuropathol (Berl) 53:203–211

Wisniewski HM, Johnson AB, Raine CS, Kay WJ, Terry RD (1970) Senile plaques and cerebral amyloidosis in aged dogs. Lab Invest 23:287–296

Wisniewski HM, Ghetti B, Terry RD (1973) Neuritic (senile) plaques and filamentous changes in aged rhesus monkeys. J Neuropathol Exp Neurol 32:566–584

Wisniewski HM, Terry RD (1973) Re-examination of the pathogenesis of the senile plaque. In: Zimmerman HM (ed) Progress in neuropathology, vol 11. Grune and Stratton, New York, pp 1–26

Wisniewski HM, Bruce ME, Fraser H (1975) Infection etiology of neuritic (senile) plaques in mice. Science 190:1108–1110

Wisniewski HM, Terry RD (1976) Neuropathology of the aging brain. In: Terry RD, Gershon S (eds) Neurobiology of aging. Raven Press, New York, pp 265–280

Wisniewski HM, Moretz RC, Lossinsky AL (1981a) Evidence of induction of localized amyloid deposits and neuritic plaques by an infectious agent. Ann Neurol 10:517–522

Wisniewski HM, Sinatra RS, Iqbal K, Grundke-Iqbal (1981b) Neurofibrillary and synaptic pathology in the aged brain. In: Johnson JE (ed) Aging and cell structure. Plenum Press, New York, pp 105–141

Wisniewski HM, Kozlowski P (1982) Evidence for blood-brain barrier changes in senile dementia of the Alzheimer type (SDAT). Ann NY Acad Sci 396:119–129

Received November 23, 1982/Accepted January 10, 1983